Optica Applicata, Vol. XXXV, No. 1, 2005

Optical beam injection methods as a tool for analysis of semiconductor structures

JAROSŁAW DOMARADZKI, DANUTA KACZMAREK

Faculty of Microsystem Electronics and Photonics, Wrocław University of Technology,
ul. Janiszewskiego 11/17, 50-372 Wrocław, Poland

Optical beam injection methods, such as an optical beam induced current (OBIC) one, have several advantages. Such methods enable a comprehensive analysis of photocurrent generated at the microregion of a semiconductor material or a device by focused light beam. In the paper, examples of applications of the OBIC method for : i) examination of the silicon *p-i-n* diodes used in a scanning electron microscope (SEM) as a detector and ii) localization of electrically active regions at the interface of the new transparent oxide semiconductor (TOS)–semiconductor structure have been outlined.

Keywords: transparent semiconducting oxide, heterojunction, *p-i-n* diode, optical beam, induced current.

1. Introduction

Manufacturing of today's microelectronic devices needs the use of novel non-destructive techniques for optical and electrical characterization of the device parameters with good spatial resolution. Suitable methods for such requirement are based on focused beam which causes induction of excess carriers in a localized region. The analysis of the current collected in the external circuit can provide important qualitative and quantitative information of the local transport properties of the device under test (DUT) [1].

Up to now, methods in which the focused light is used in order to generate carriers for semiconductor investigations have been applied in many variations. There also exist many names such as: light/laser beam induced current (LBIC) [2], optical beam induced current (OBIC) [3], infrared beam induced current (IRBIC) [4], monochromatic beam induced current (MBIC) [5] and others, but all of them describe the same method. From experimental point of view, of major importance is the way how the induced current is collected. As has been presented in Fig. 1, there is a common difference depending on whether the signal measured was taken at a short (contacts A and C) or an open (contacts A and B) junction. In both cases focused and modulated light beam is scanned across the semiconductor sample and generates electron-hole pairs in localized area. If this localized region has any electrical field (*i.e.*, junction or

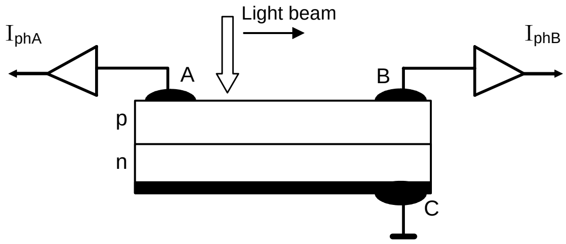

Fig. 1. Schematic diagram of beam induced current phenomena in the case of planar *p-n* junction; A, B, C – ohmic contacts, I_{ph} – photocurrent.

electrically active region caused by defects), the charges will be separated and the induced current will flow between two remote contacts.

A short circuit current configuration has been especially applied in investigations of *p-n* junction based devices, such as: solar cells [6], photodetectors [7], and silicon wafers [8]. Based on the photocurrent measured it is possible to calculate quantum efficiency of the device as well as other parameters such as: diffusion length, surface recombination velocity or lifetime of minority carriers [9].

Although the open circuit configuration was first applied in the middle of the 1980's [10], up to now there has not been developed any consistent theory which would allow electrical parameters to be determined on the basis of photocurrent measured in this case. Few exceptions, for example, include measurement of the junction depth, as was reported by the group of MUSCA *et al.* [11]. A great advantage of the open circuit configuration was that it allowed simultaneous investigation of multiple structures fabricated at the same wafer using a single connection.

In the present work, tests of the *p-i-n* diodes were carried out in order to enable the choice of detectors with similar electrical parameters. These detectors are most commonly used in multidetector system for backscattered electrons (BSE) in a scanning electron microscope (SEM).

Additionally, the examination of electrically active areas at the interface of the transparent semiconducting oxide–semiconductor by applying the OBIC method has been outlined. The semiconducting thin film oxide was based on the titanium dioxide lattice doped with transition metals and manufactured by a modified magnetron sputtering method [12, 13]. As a substrate well conducting (*n*-type) silicon wafers have been used.

2. Experimental set up

In our experimental set up (Fig. 2) an OPTEL monochromator, remotely controlled by PC equipped with a 450 W xenon lamp has been used as a light source. Owing to this the experiment can be done at different wavelength of incident light beam ranging from 2×10^{-7} m to 24×10^{-7} m with the minimum wavelength step of 1.5×10^{-10} m.

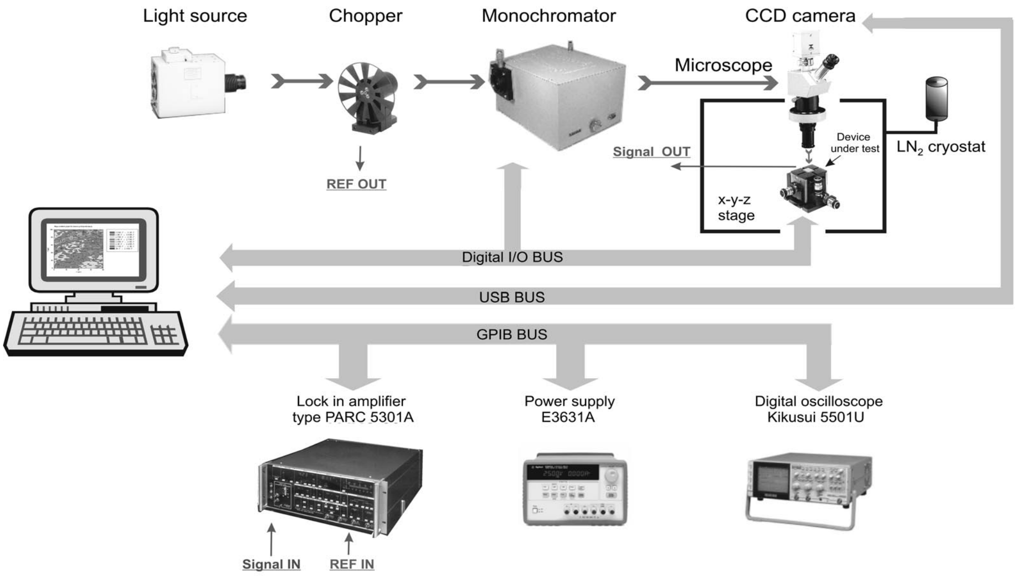

Fig. 2. Schematic block diagram of the measurement system used in our OBIC method.

Besides the power and the wavelength of the incident light beam also the spot size has to be taken into account [14]. At first, the light is chopped and illuminates a 3×10^{-4} m pinhole. Then, the beam is focused with the help of optical lenses onto the sample surface of about 35×10^{-6} m (or less) in diameter.

The optical system has been equipped with a digital CCD camera connected with the host computer via USB (universal serial bus) interface. Thanks to this, both the scanning area selected in the experiment and the actual position of the scanning beam can be observed directly on the computer screen. A digital image of the light reflected from the surface of the device under test (DUT) can be achieved and stored. DUT is placed on a remotely controlled *x*-*y*-*z* stage. To obtain an image, the current induced must be measured step by step at each point of selected area. A high signal to noise ratio is assured by a lock-in technique application. The lock-in type amplifier (EG&G PARC 5301A type) measures the magnitude of generated photocurrent and the phase -shift between this current and reference signal. The digitized values are sent via the GPIB (IEEE-488.2) interface to PC and stored in a file as a function of incident light position. The minimum step size in the applied system amounts to 2.5×10^{-6} m. The data is plotted as 2D gray scale or colour images with custom palette. Both the magnitude and phase-shift images can be obtained. The control system was implemented in the TestPoint environment working under Windows. The set of equipment used allows one to make a full-automated measurement and data acquisition.

3. OBIC application

Focused optical beam injection methods enable comprehensive analysis of photocurrent generated in the microregion of semiconductor and on the basis of collected data 2D grey scale or colour images can be created [14, 15]. This may be useful in detection of defects with very poor electrical activity [3, 16].

3.1. Analysis of SEM detectors

In Figures 3 and 4, exemplary distribution maps of the magnitude of induced current measured on silicon *p*-*i*-*n* type photodiode in the case of different connection configurations have been presented. In Fig. 3, the induced current was obtained in the case of the open circuit current collected between A and B contacts. The magnitude of collected current strongly depended on the position of incident light beam *vs*. remote contacts. Near the centre of the structure being analysed photocurrent decreased to

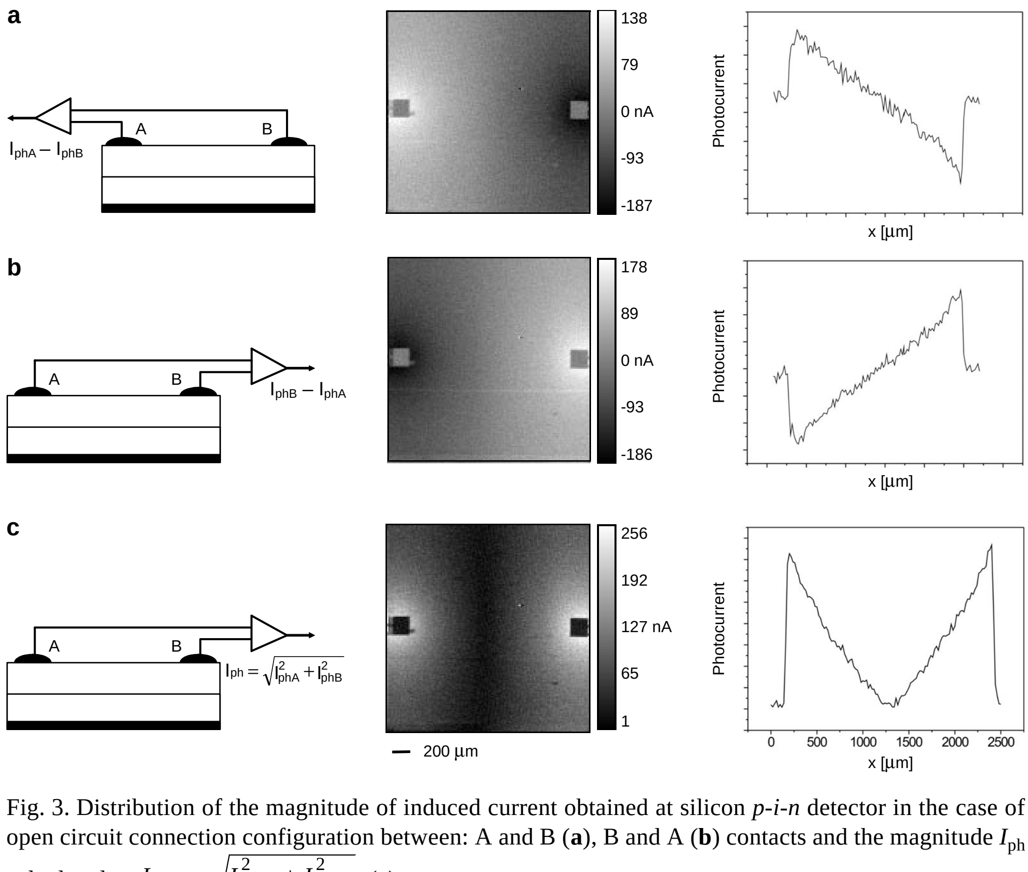

Fig. 3. Distribution of the magnitude of induced current obtained at silicon *p*-*i*-*n* detector in the case of open circuit connection configuration between: A and B (**a**), B and A (**b**) contacts and the magnitude I_{ph} calculated as $I_{ph} = \sqrt{I_{phA}^2 + I_{phB}^2}$ (**c**).

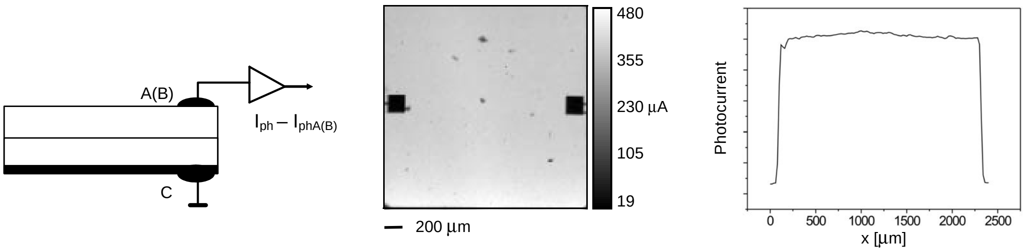

Fig. 4. Distribution of the magnitude of the induced current obtained at silicon *p-i-n* detector in the case of short junction connection configuration.

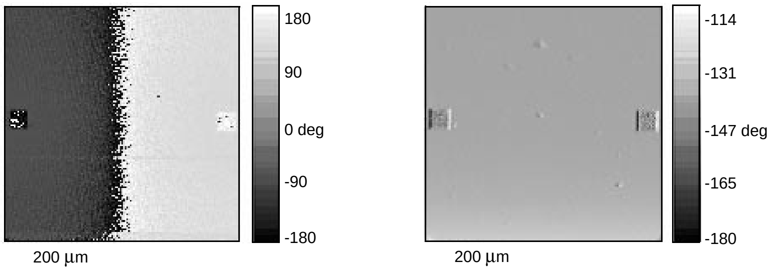

Fig. 5. Distribution maps of phase shift between measured current and reference signal in the case of the connection configuration as: **a** – in Fig. 3**c**, and **b** – in Fig. 4.

zero. The polarity of the current measured depends on whether a signal was collected at A or B contact. In Fig. 3**c** the magnitude of collected current calculated as $I_{ph} = \sqrt{I_{phA}^2 + I_{phB}^2}$ is presented.

In Figure 4, a short junction configuration is presented and the current is collected between A (or B) and C contacts. The photocurrent has quite a uniform distribution over the area under investigation. The visible darker spots are due to the surface impurities of the structure being tested.

Figure 5 presents a distribution of phase shift between measured photocurrent and the reference signal in the case of different connection configuration in the OBIC method. Similarly to the image presented in Fig. 4, Fig. 5**b** shows a uniform distribution of measured quantity over investigated area. Pinholes correspond to the same surface impurities which can also be observed in Fig. 4. The phase shift in Fig. 5**a** has changed near the centre of the structure, which indicates change of the direction of collected current (see Fig. 3).

Experiments described above in the case of open and short circuit current were performed without any additional external electric field. The current could be observed thanks to the photogenerated excess minority carriers separated directly at the *p-n* junction of the detectors being tested. Besides the nature of collected current it is worth noting that measured signal in Fig. 4 was about two orders of magnitude higher than in the case of signal in Fig. 3.

3.2. Analysis of the transparent semiconducting oxide–semiconductor interface

A new kind of structure with nanocrystalline titanium dioxide-based semiconducting thin films was manufactured using a low-pressure hot target reactive magnetron sputtering process [12]. As dopants a V and Pd sheets have been co-sputtered from Ti target in order to obtain Ti-V-Pd oxide compositions. The amount of dopants has been estimated at V = 10.6 at.%, Pd = 6.67 at.%. The thickness of the fabricated films, measured by optical interference method with Hg (551 nm) filtered lamp was 395 nm.

In order to make electrical measurements, the Ag/$Ti_{10}W_{90}$ electrode with a diameter of 3 mm was evaporated through the mask in the layer under examination. At the backside of silicon wafer an ohmic contact has been made using In-Ga eutectic alloy. A schematic drawing of the structure under test is presented in Fig. 6.

In Figure 7**a**, characteristics obtained from the measurement of $i_{ph}(x)$ photocurrent generated during a single scan of light beam through the range of analysed structure: electrode–thin oxide film–silicon substrate (Me/(Ti-V-Pd) oxide/Si) are presented. Below the characteristics, a general view of the structure is shown.

The measurements were carried out at room temperature at the wavelength $\lambda = 660$ nm, for which the thin film is permeable at different values of supply voltage (U_{bias}). The increase in the amplitude of photocurrent, registered in the junction range: thin oxide film–silicon substrate, confirms the presence of the built-in potential (space charge), ensuring the separation of generated current carriers. Based on the characteristics shown in Fig. 7 it can be noticed that the location of electrically active range corresponds to dimensions of analysed structure. Similarly to the case of conventional semiconductor junctions, the increase in bias voltage results in extension of space charge range. This is confirmed by the fact that at the boundary: thin Ti-V-Pd oxide film–silicon substrate, the junction has been formed. Additionally, the

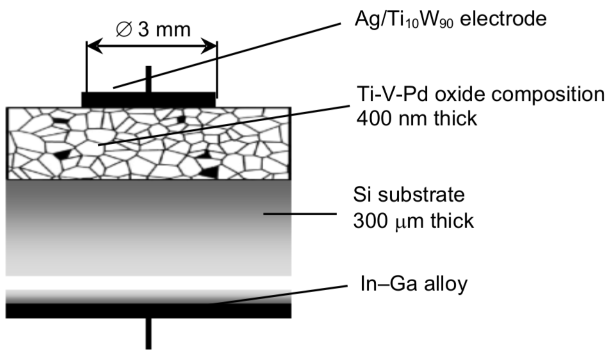

Fig. 6. Schematic drawing of the structure under test.

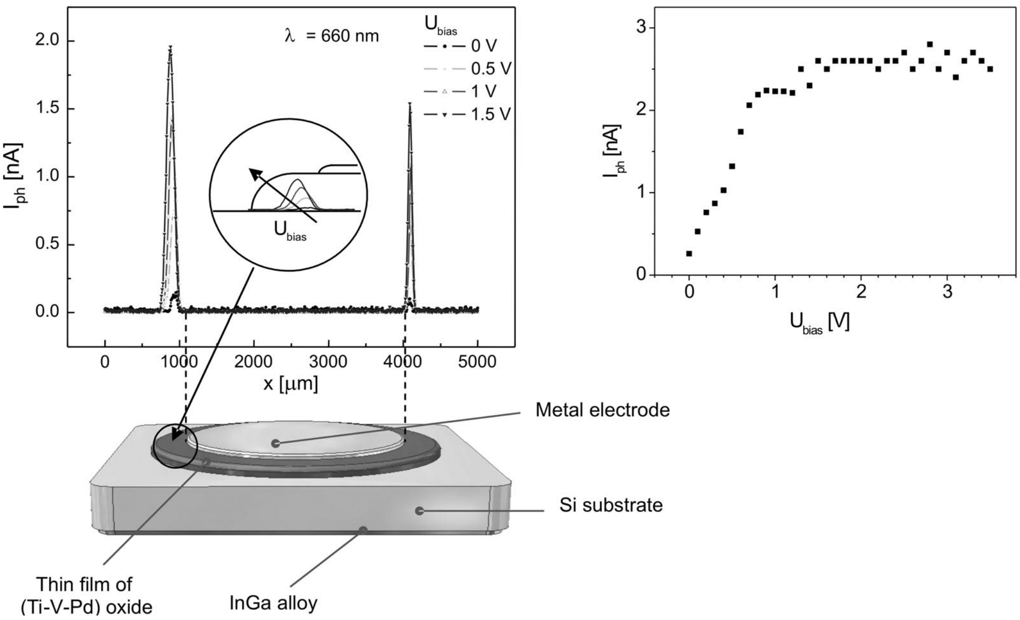

Fig. 7. Characteristics of photocurrent $i_{ph}(x)$: **a** – obtained in effect of single scan of light beam across the area of Me/(Ti-V-Pd)/Si structure and **b** – *vs*. polarisation bias (U_{bias}). Light beam parameters: diameter ca. 35 μm, frequency of modulation f = 182 Hz. The characteristics were taken at room temperature with the wavelength of λ = 660 nm in the case of short junction connection configuration.

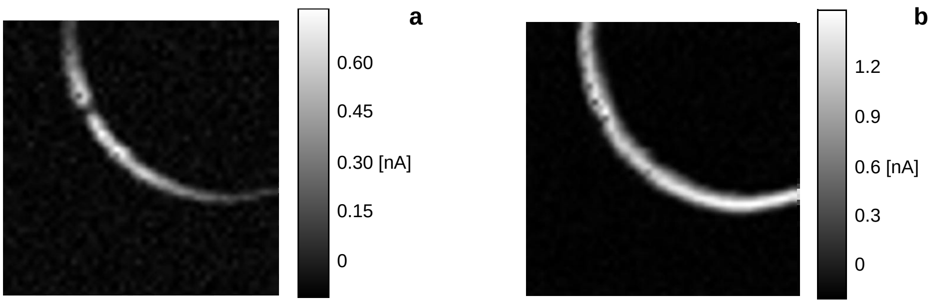

Fig. 8. Map of photocurrent distribution at the boundary: semiconducting oxide–Si of Me/(Ti-V-Pd) oxide/Si structures determined at the bias voltage: **a** – U_{bias} = 0 V, **b** – U_{bias} = 1 V.

increase in the value of measured photocurrent with increase in bias voltage is presented in Fig. 7**b**.

Distribution of space charge can also be observed on 2D maps of measured photocurrent, as is shown in Fig. 8. The maps were obtained by point-by-point measurement of photocurrent generated in the selected area scanned with the light beam upon selected polarisation bias.

Photocurrent presented in Figs. 7 and 8, was collected in the short circuit current configuration. This type of connections allowed us to collect the photogenerated current in a simple way with a high sensitivity (a high signal to noise ratio).

The results described above seem to be very attractive for novel applications of this kind of structures in microelectronics. For example, as we have already shown in [13], they could be applied in a new kind of photodevices.

4. Conclusions

Optical beam induced current method (OBIC) has proven to be very useful in the diagnostics of typical semiconductor detectors as well as analysis of the new kind of structures with the electrically active region at the interface of semiconducting metal oxide thin film deposited on silicon substrate.

Characteristics scanned “in-line” allow us to indicate the electrically active regions which were equal to physical dimensions of the structure analysed. Similar to the conventional junction based structures, the distribution of measured photocurrent at the fabricated heterojunction of semiconducting oxide–semiconductor was found to be dependent on external polarisation bias.

The photoelectric effect revealed on the boundary of thin semiconducting oxide layer with silicon substrate by OBIC method seems to be very interesting. From the subject literature [17] it follows that thin semiconductor films produced on the basis of oxides are highly desired. In the the authors’ opinion, the connection of the films with conventional semiconductor materials, like silicon, which are widely used in electronics, should lead in the nearest future to the fabrication of new types of microelectronic devices.

Acknowledgment – This work was supported by the State Committee for Scientific Research (KBN) in the years 2004–2005.

References

[1] CHAN D., PHANG J., CHIN J., KOLACHINA S., *Single contact beam induced current phenomena – a review*, Diffusion and Defect Data Pt. B: Solid State Phenomena **78-79** (2001), pp. 11–8.

[2] ACCIARRI M., BINETTI S., RACZ A., PIZZINI S., AGOSTINELLI G., *Fast LBIC in-line characterization for process quality control in the photovoltaic industry*, Solar Energy Materials and Solar Cells **72**(1-4), 2002, pp. 417–24.

[3] CASTALDINI A., CAVALLINI A., POLENTA L., *Optical beam induced current investigations of particle detectors*, Physica Status Solidi B **222**(1), 2000, pp. 245–50.

[4] ASTAFIEV O.V., KALINUSHKIN V.P., YURYEV V.A., *Scanning mid-IR-laser microscopy: An efficient tool for materials studies in silicon-based photonics and photovoltaics*, Journal of Crystal Growth **210**(1-3), 2000, pp. 361–5.

[5] SHIMOKAWA R., TAJIMA M., WARASHINA M., KASHIWAGI Y., KAWANAMI H., *Correspondence among PL measurement, MBIC measurement and defect delineation in polycrystalline cast-Si solar cells*, Solar Energy Materials and Solar Cells **48**(1-4), 1997, pp. 85–91.

[6] GALLOWAY S.A., EDWARDS P.R., DUROSE K., *Characterisation of thin film CdS/CdTe solar cells using electron and optical beam induced current*, Solar Energy Materials and Solar Cells **57**(1), 1999, pp. 61–74.

[7] CASTALDINI A., CAVALLINI A., POLENTA L., NAVA F., CANALI C., *Electric field distribution in irradiated silicon detectors*, Nuclear Instruments and Methods in Physics Research, Section A Accelerators, Spectrometers, Detectors and Associated Equipment **476**(3), 2002, pp. 550–5.

[8] MARTINUZZI S., HENQUINET N.G., PERICHAUD I., MATHIEU G., TORREGROSSA F., *Efficiency of cavity gettering in single and in multicrystalline silicon wafers*, Materials Science and Engineering B: Solid State Materials for Advanced Technology **B71**(1-3), 2000, pp. 229–32.

[9] GEIGER P., HAHN G., FATH P., BUCHER E., *Comparing improved state-of-the-art to former EFG Si-ribbons with respect to solar cell processing and hydrogen passivation*, Solar Energy Materials and Solar Cells **72**(1-4), 2002, pp. 155–63.

[10] BAJAJ J., BUBULAC L.O., NEWMAN P.R., TENNANT W.E., RACCAH P.M., *Spatial mapping of electrically active defects in HgCdTe using laser beam-induced current*, Journal of Vacuum Science and Technology A: Vacuum, Surfaces, and Films **5**(5), 1987, pp. 3186–9.

[11] MUSCA C.A., REDFERN D.A., SMITH E.P., DELL J.M., FARAONE L., BAJAJ J., *Junction depth measurement in HgCdTe using laser beam induced current (LBIC)*, Journal of Electronic Materials **28**(6), 1999, pp. 603–10.

[12] DOMARADZKI J., PROCIOW E., KACZMAREK D., *Ti Zr dielectric layers deposited by hot target reactive magnetron sputtering*, [In] *ASDAM'02. Conference Proceedings. Fourth International Conference on Advanced Semiconductor Devices and Microsystems*, [Eds.] Breza J., Donoval D., IEEE, Piscataway, NJ, USA 2002, pp. 47–50.

[13] DOMARADZKI J., PROCIOW E., KACZMAREK D., BERLICKI T., KUDRAWIEC R., MISIEWICZ J., MIELCAREK W., *Structural, optical and electrical characterization of Co-Pd doped* TiO_2 *semiconducting thin films sputtered on silicon*, Optica Applicata **33**(4), 2003, pp. 661–668.

[14] DOMARADZKI J., *Light-beam-induced current (LBIC) technique for semiconductors and ICs testing*, Proceedings of the SPIE **5064**, 2003, pp. 269–74.

[15] DOMARADZKI J., KACZMAREK D., WĘGRZECKI M., WĘGRZECKA I., BUDZYŃSKI T., KRZEMIŃSKI S., GRABIEC P., *Detectors of optical and nuclear radiation examined by the light-beam-induced current (LBIC) method*, Proceedings of the SPIE **5064**, 2003, pp. 275–80.

[16] BERLICKI T., OSADNIK S., PROCIÓW E., *Thermal sensors with controlled sensitivity*, [In] Proceedings of XXIV International Conference IMAPS'00, Rytro 2000, p. 365.

[17] VAN DE KROL R., TULLER H.L., *Electroceramics – the role of interfaces*, Solid State Ionics, Diffusion and Reactions **150**(1-2), 2002, pp. 167–79.

Received September 23, 2004